INDIAN JOURNAL OF SCIENCE AND TECHNOLOGY

RESEARCH ARTICLE

OPEN ACCESS
Received: 17-08-2024
Accepted: 22-09-2024
Published: 04-11-2024

Citation: Ashok P, Kumar RU, Gopal D, Jagadha S, Reddy MCK (2024) Influence of Higher Order Chemical Reaction on Rotational and Permeable Radiative Flow with Interruption of Micro-organism. Indian Journal of Science and Technology 17(41): 4250-4261. https://doi.org/10.17485/IJST/v17i41.2671

* **Corresponding author**.
ashokpiitkgp@gmail.com

Funding: None

Competing Interests: None

Published By Indian Society for Education and Environment (iSee)

ISSN
Print: 0974-6846
Electronic: 0974-5645

Influence of Higher Order Chemical Reaction on Rotational and Permeable Radiative Flow with Interruption of Micro-organism

P Ashok[1]*, Rama Udai Kumar[2], D Gopal[3], S Jagadha[4], M Chenna Krishna Reddy[1]

1 Department of Mathematics, UCS, Osmania University, Hyderabad, 500007, Telangana, India
2 Department of Mathematics,, Pallavi Engineering College, Kuntloor, Hyderabad, 501505, Telangana, India
3 Junior Lecturer in Mathematics, Telangana Tribal Welfare Upgraded Residential Junior College for Boys, Cheemanpally, Nizamabad, 503165, Telangana, India
4 Department of Mathematics,, Institute of Aeronautical Engineering, Dundigal, Hyderabad, Telangana, India

Abstract

Objective: The concentration on the function of the non-Newtonian radiative Casson Nanofluid model via a permeable and stretchable cone has been investigated. The innovation of the problem is Casson, taken as base fluid, and Manganese Ferrite is dropped in the base fluid under the action of a higher-order chemical reaction. This study examines the convective magneto-hydrodynamic (MHD) flow of a conducting micro-organism fluid confined within a horizontal channel via stimulus of a transverse magnetic field (MHD) and thermal radiation parameter. **Methods:** The foremost partial differential equations (PDE) are changed into an arrangement of ordinary differential equations by applying adequate corresponding transform. The outputs of these equations are performed numerically employing the RK method and computed by well-established BVP4C MATLAB software Special features such as radiation, heat generation/absorption, Joule heating, and electrically conductive MHD are examined. Skin friction and Nusselt number are incorporated into the flow and results are tabulated and outcomes are discussed graphically. **Findings:** The system incorporates the effects of micro-organism, pressure gradient and the movement of the moving cone. The generated heat is significant enough to cause radiation from both the fluid and the dust particles. Solutions for velocity and temperature distributions of the fluid, as well as the velocity and energy of the dust particles, are obtained using a perturbation scheme. The analytical impact of numerous geometrical parameters on both fluid and dust particle profiles has been analyzed and illustrated graphically. The impact of nonlinear partial derivative formulations is developed subjected to boundary layer theory. **Novelty:** As labelled in the results, heterogeneous is the examination of thermal radiation in science and technology such as liquid metal fluids different momentum devices for missiles, and turbines of gas effects on thermal radiation are exhibited and distinguished in various investigations and mathematical applications uses of the view in which radiant production be dependent on temperature are point out as a new value to the prevailing literature.

Keywords: Thermal radiation; Brownian motion; Buoyancy flow; Chemical reaction; Heat and Mass transfer; Rotating cone

1 Introduction

The investigation on governing flow and energy transportation is highlighted by many researchers for Casson fluid motion due to its significant part in industrial applications. The rheological characteristics of non-Newtonian Casson fluid are the association between shear stress and strain. The applications of shear-thinning are suitable for Casson fluid due to its shear viscosity and stress. The noted examples of Casson fluid are honey, jellies, and soups. Narsimha Reddy et al.[(1)] examined the movement of Casson nanofluid across an unstudied electrically conductive MHD flow problem. The geometrical model has a stretchable sheet and non-dimensional parameters such as Joule heating and radiation are examined. Moatimid et al.[(2)] proposed the conical gap among rotating surfaces and horizontal discs to the nanoparticles of Casson fluid flow. Aamir et al.[(3)]addressed the performance of Casson nanofluid over a thin indicator. They examined the aiding and opposing force of buoyancy in the two-dimensional mixed convective medium.

The investigation reported that the proportion of heat transfer is dependent on the thickness of the needle. The essential practical application of rotating stretchable domains is astronomy and material sciences. An excellent research work has been prepared to know about rotating stretchable flow problems by Aisha et al.[(4)]. The detailed study of viscosity and nanoparticles, that is, ethylene glycol as dishonourable fluid and Titanium nanoparticles are deferred in the dishonourable fluid. Vinod Kumar et al.[(5)] calculated the Cattaneo-Christof model on a stretchable porous sheet and analyzed Maxwell nanofluid flow incorporating advanced order chemical reaction, radiative MHD, and viscous dissipation. The research witnessed graphically that the concentration gradient declines with an upsurge of a chemical reaction.

The electrostatic filters, power pumps, and heat exchanges are the devices, activated by forces of Magneto-hydrodynamics functioning. The magnetic field possesses the resistive Lorentz force to decline fluid motion and enhance concentration and temperature distribution. Thus, MHD plays a vital role in boundary layer separation. Jyoti Das et al.[(6)] explored unsteady MHD governing flow via an oscillating perpendicular external of the Darcy model. The vertical solid body is rotational and influenced chemically. Punith et al.[(7)] reviewed the improved Fourier heat flux model and tests were performed on a curved stretching sheet. Khan et al.[(8)] studied heat and mass transportation analysis for the model of Williamson MHD nanofluid via strained sheet and permeable layer.

In this research paper, we are outlining a two-dimensional Casson Nanofluid via a stretchable surface under the actions of Ohmic dissipation. The dimensionless parameter Joule heating is characterized over a sheet. The heat transportation is executed on a shrinkable sheet. Abideen et al.[(9)]tested here impacts of radiation and heat generation on Casson nanofluid over a stretchable curved surface. The dual nature of carbon nanotubes, single as well as numerous enclosed carbon nanotubes are dropped in the base fluid, blood are demonstrated in detail in this study. Many research scholars demonstrated about connectivity of nanoparticles with dimensionless parameters.

The chemical processing has numerous applications in the engineering field and geophysics. The cooling of nuclear reactors, thermal insulation, and drying of porous solids are the successful steps of application of flow reactions chemically. Sharma et al.[(10)] deliberated higher order chemical reactions influenced by velocity slip, thermal slip, concentration slips and magnetic strength as external forces at an inclined position of the model. Gopal et al.[(11)] discussed viscous and joule heating effects on Casson Nano-fluid at an inclined magnetic field. The model is performed on a stretchable sheet associated with multiple slip boundary layer conditions. Jagadha et al.[(12)]focused on micro polar non-Newtonian fluid influenced by MHD, suction/blowing, heat generation, thermophoresis and chemical quantifiers.

Rehman et al.[(13)] addressed artificial intelligence to examine Williamson fluid flow and the report indicated that neural network analysis has a successful platform for magnetized surfaces. Raghavendra et al.[(14)] observed MHD Casson nanofluid electrically and reported on the impacts of radioactivity, higher order chemical reaction. Jan et al.[(15)] focused on detailed modelling of chemical reaction arrangements consuming incline constructions. The pertinent model parameters connected to physical assumptions, equations governing the flow and energy as well as spices movement are examined. Recently Muhammad et al.[(16–20)] has studied various fluids of Carreau, Cattaneo-Christov, Maxwell fluid, Darcy-Forcheimer, and Lorentz forces with impacts of microorganisms through various channels.

The present framework is predictable to obtain an enhanced physical significance of the flow processing, which will guide the strategy of the governing flow. We have explored energy transport through a radiative and heat generation of Casson non-newtonian nanofluid via a stretchable sheet. According to the literature survey in detail, a combination of higher-order chemical reactions and electrically conductive MHD has never been explored before. The exploration has been categorized into distinctive portions. The first serving reveals mathematical construction and the second portion elaborates on the mathematical solutions computed by employing the numerical technique RK method via BVC Software. The last part shows the physical significances of dimensionless parameters are illustrated graphically.

2 Mathematical Formulation

In this investigation, we summarized chemical reaction and thermal radiation, infusion-induced revolution position around slender bodies with the influence of buoyancy transportation phenomena. Here exposed temperature of the surroundings unvarying at T_w, exceeds the temperature acquires the unvarying value T_∞ observe from the surface far away and the flow's structure. The cylindrical system represents the direction of (x, r), the vertex of the boy located at the origin. The concentration of the outward is taken unvaryingly $C_w$and that of ambient fluid has occupied at C_∞. The coordinate denotes the equilibrium distance between numerous forms of slender revolutions and vertical to the rotating slender surface. The governing equation from Figure 1 is described by Bhatti et al.[(21)] phenomena incorporating Boussinesq approximations.

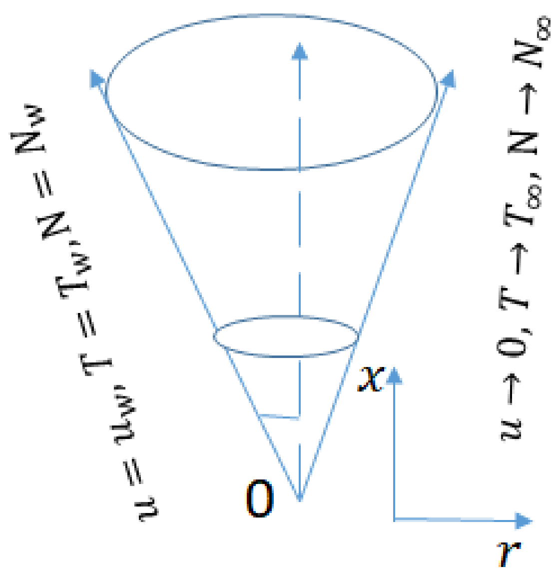

Fig 1. Problem of the geometrical flow model

$$(ru)_x + (rv)_r = 0 \tag{1}$$

$$\frac{1}{r}(\psi)_r = (Kg/\upsilon)\left(\beta_T(T - T_\infty) + \beta_C(C - C_\infty)\right) \tag{2}$$

$$(T)_x(\psi)_r - (T)_r(\psi)_x = \alpha\Big(r(T)_r\Big)_r + (q_r)_z + (r\tau)\Big((D_T/T_\infty)\Big((T)_r\Big)^2 + D_B(T)_r(C)_r\Big) \tag{3}$$

$$(C)_x(\psi)_r - (C)_r(\psi)_x = D_B\Big(r(C)_r\Big)_r + (D_T/T_\infty).\Big(r(T)_r\Big)_r - K.(C - C_\infty)^n \tag{4}$$

$$(N)_x(\psi)_r - (N)_r(\psi)_x + (bw_c/C_\infty)\Big((N(C)_r)_r\Big) = D_n\Big(r(N)_r\Big)_r \tag{5}$$

Here Boussinesq approximation has been expressed as

$$(\rho/\rho_\infty) = 1 - \beta_T(T - T_\infty) - \beta_C(C - C_\infty) \tag{6}$$

The existing governing boundaries are:

At, $r = R(x)$

$$\upsilon = 0, T = T_w(x) - T_\infty = Ax^{(a)}, C = C_w(x) - C_\infty = Bx^{(b)}, N = N_w(x) = Nx^{(c)} \tag{7}$$

At infinity place

$u = 0, T = T_\infty, C = C_\infty, N = N_\infty Atr \to \infty$

Here assessment of the thermal radiation parameter has been expressed as

$$q_r = -\frac{4\gamma^*}{3k^*}.\frac{\partial T^4}{\partial r} \tag{8}$$

T^4has expressed as utilizing a Taylor series via at-temperature $T_\infty$and discounting complex order express results as.

$$T^{(4)} = 4TT_\infty^{(3)} - 3T_\infty^{(4)} \tag{9}$$

Recollecting Equations from Equation (9) in Equation (8), Equation (3) Produce

$$(T)_x(\psi)_r - (T)_r(\psi)_x = \alpha\left(1 + (4/3)Nr\right).\Big(r(T)_r\Big)_r + r\tau\Big(D_T/T_\infty\Big((T)_r\Big)^2 + D_B(T)_r(C)_r\Big) \tag{10}$$

Here thermal radiation is defined as$Nr = \frac{4\gamma^* T_\infty^{(3)}}{kk^*}$and also the expectation of the similarity variable with non-dimension functions defined as $f(\eta), \theta(\eta), \phi(\eta)$ and $\chi(\eta)$.

$$\begin{gathered} \eta = Ra\left(\frac{r}{x}\right)^2, \ Ra = \frac{Kg\beta_T(T_w - T_\infty)x}{\alpha\upsilon}, \ u = \left(\frac{1}{r}\right)(\psi)_r, v = \left(-\frac{1}{r}\right)(\psi)_r, \ \psi = (\alpha x)f(\eta), \\ T - T_\infty = \theta(\eta)(T_w - T_\infty), \ C - C_\infty = \phi(\eta)(C_w - C_\infty), \ N - N_\infty = \chi(\eta)(N_w - N_\infty) \end{gathered} \tag{11}$$

Here defines the stream function ψ, Ra—denotes reformed local Rayleigh number,

Here assessment of $\eta = \eta_0(\eta_0$ denotes stable constant) and it shows that an arithmetically small value of a revolution of body, consideration of both the size and shape of the slender revolution, has been expressed from Equation (10) invented.

$$R(x) = \left(\frac{\upsilon\alpha\eta_0}{Kg\beta_T A}\right)^{1/2} x^{\left(\frac{1-a}{2}\right)}$$

Here applied scenarios show the parameter $'a'$must fallows to $a \leq 1$for real-world relevance. For occurrence of insurgency results from a cone-shaped resembles $a = -1$,while a parabolic of rebellion parallels to $a = 0$.

The system of governing equations transformed as:

$$f^{'}(\eta) = \frac{1}{2}(\theta(\eta) + Nc\phi(\eta))$$

$$\left(1 + \frac{4}{3}Nr\right)\theta^{''\frac{1}{2}\left(af^{'}(\eta)\theta(\eta) - f(\eta)\theta^{'}(\eta) - 2\theta^{'}(\eta)\right)\left(Nb\theta^{'}(\eta)\phi^{'}(\eta) + Nt\theta^{'}(\eta)^{2}\right)}$$

$$\phi^{''\frac{1}{2}\left(bLef^{'}(\eta)\phi(\eta) - Lef(\eta)\phi^{'}(\eta) - 2\phi^{'}(\eta) - \frac{2}{Le}\left(\frac{Nt}{Nb}\right)\left(\theta^{'}(\eta) + \theta^{''}()^{n}\right)()\right)}$$

$$\chi^{''\frac{1}{2}\left(cLef^{'}(\eta)\chi(\eta) - Lef(\eta)\chi^{'}(\eta) + pe\begin{pmatrix}\chi(\eta)\phi'(\eta) + 2\phi\chi'\eta \\ +2\eta\chi(\eta)\phi^{''}\end{pmatrix}0\right)}$$

The transformed boundary conditions are:

$$\eta = \eta_0, f(\eta) + (a_1 - 1)\eta f^{'}(\eta) = 0, \theta(\eta) = 1, \phi(\eta) = 1, \chi(\eta) = 1$$

$$\eta \to \infty, f^{'}(\eta) = 0, \theta(\eta) = 0, \phi(0) = 0, \chi(\eta) = 0$$

Here, $Nc = \frac{\beta_{c1}(C_w - C_\infty)}{\beta_{T1}(T_w - T_\infty)}$the ratio of buoyancy,

$Nb = \frac{D_B\tau(C_w - C_\infty)}{\alpha}$the Brownian parameter,

$Nt = \frac{D_T\tau(T_w - T_\infty)}{T_\infty\alpha}$ thermophoresis constant,

$Le = \frac{\alpha}{D_B}$Lewis number,

$pe = \frac{bw_c}{D_n}$ Peclet number.

Here limitations depiction shows in the real world are the constants related to thermal and diffusion transmission, as these values are expressed.

$$Nu = \frac{hy}{k} = -\left(\left|\frac{\partial T}{\partial r}\right|_{r=R(x)}\right)/(T_w - T_\infty) = -2\eta_0^{0.5}Ra^{0.5}\theta^{'}(\eta_0)$$

$$Sh = \frac{mx}{D_B(C_w - C_\infty)} = -2\eta_0^{0.5}Ra^{0.5}\phi^{'}(\eta_0)$$

$$NSh = \frac{mx}{D_B(N_w - N_\infty)} = -2\eta_0^{0.5}Ra^{0.5}\chi^{'}(\eta_0)$$

3 Introduction to Runge-Kutta Method

The Runge-Kutta system is extensively used and an effective system for numerally solving differential equations for the initial-value problems.

Implementing special variable notations to convert higher-order formulated equations into linear differential equations.

$$f = f_1, f^{'} = f_2, f^{"} = f_3, g = f_4, g^{'} = f_5, \theta = f_6, \theta^{'} = f_7, \phi = f_8, \phi^{'} = f_9,$$

$$f_3 = \frac{1}{\phi_2}\left(\frac{\beta}{1+\beta}\right)\left[K_1 f_2 \phi_2 - \phi_1\left(f * f_3 - f_2\hat{2} - F_1 * f_2\hat{2} + 2K\hat{2} f_4\right) - \phi_3 Ha\hat{2}\left(E_1 - f_2\right)\right]$$

$$f_5 = \frac{1}{\phi_2}\left(\frac{\beta}{1+\beta}\right)\left[K_1 f_4 \phi_2 + \phi_1\left(f_2 * f_4 - f_1 * f_5 - F_1 * f_4 + 2K\hat{2} f_2\right) - \phi_3 Ha\hat{2}\left(E_1 - f_4\right)\right]$$

$$f_9 = -Sc\left[f_1 * f_8 + \Gamma f_8\hat{n}\right]$$

The non-dimensional quantifiers are the replica of the physical insight of Casson Magnese ferrite nanofluid flow, MATLAB software is used to present the numerical outputs graphically.

4 Results and discussion

The velocity, temperature, micro-organism and concentration profiles are acquired by the equations of Equations (6), (7), (8) and (9) with the boundary conditions Equation (10) transferred by mathematical values to the parameter that comes across in the problem. Here our target is to report the features of distinct variables like Lewis number (Le), Peclet number (Pe), Brownian motion parameter (Nb), Ratio of Buoyancy (Nc), thermal radiation (Nr), Thermophoresis Parameter (Nt) on velocity $\left(f^{'}\right)$, temperature (θ), and concentration (φ), and Micro-organism (χ). The resulting systems consisting of Equations (6), (7), (8) and (9) through boundary conditions Equation (10) have been elucidated systematically by utilizing the Runge-Kutta technique. Mathematical values are communicated in relation to graphical to investigate the impact of several flow, monitoring parameters.

Generally, at the boundary layer, fluid is heated by Brownian motion support with immediately moderate particle deposition away from the fluid on the surface. In Figure 3 the evolution of concentration with variation in buoyancy parameter Nc depicts, Boosts flow velocity and escalations the momentum boundary layer thickness. It is apparent that the concentration reductions with an escalation in buoyancy parameters and the thermal boundary layer are reduced.

The fraction of thermal diffusivity and mass diffusivity is known as as Lewis Number (Le). Elevated values of Lewis number(Le) leads to ascent in both concentration (Figure 4) and micro-organism profile (Figure 5). From Figure 6 and Figure 7 ascent values of (γ) rises with influences of the fluid velocity and micro-organisms in both cases. It is perceived that the growing values of chemical reaction parameters reduce the concentration of the kinds at the boundary layer. This means that chemical reactions in this arrangement have consequences for the consumption of chemicals, due to this occurrence results in a reduction in the temperature profile (Figure 8) and an increase in the micro-organism (Figure 9) profile.

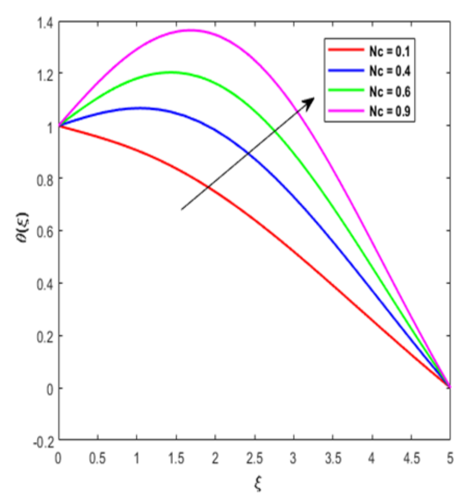

Fig 2. Stimulation of Buoyancy parameter$(Nc = \mathbf{0.1}, \mathbf{0.4}, \mathbf{0.6}, \mathbf{0.9})$ $on\ \theta(\xi)$

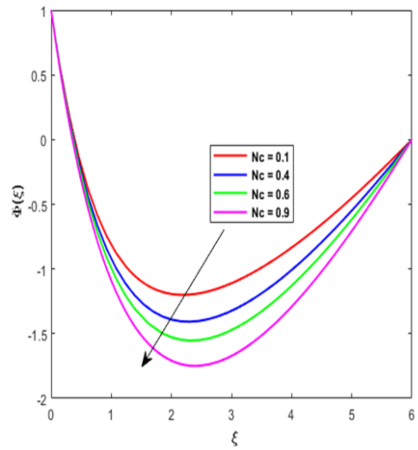

Fig 3. Stimulation of Buoyancy parameter$(Nc = \mathbf{0.1}, \mathbf{0.4}, \mathbf{0.6}, \mathbf{0.9})$ on $\phi(\xi)$

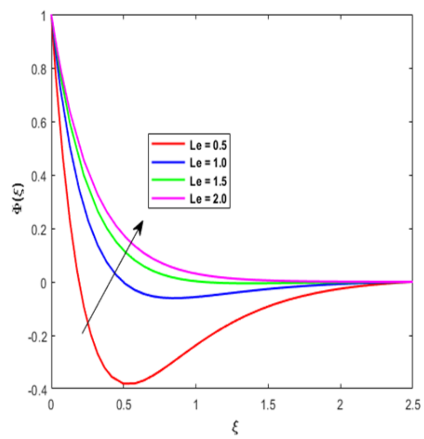

Fig 4. Stimulation of Lewis number $(Le = \mathbf{0.5}, \mathbf{1.0}, \mathbf{1.5}, \mathbf{2.0})$ on $\phi(\xi)$

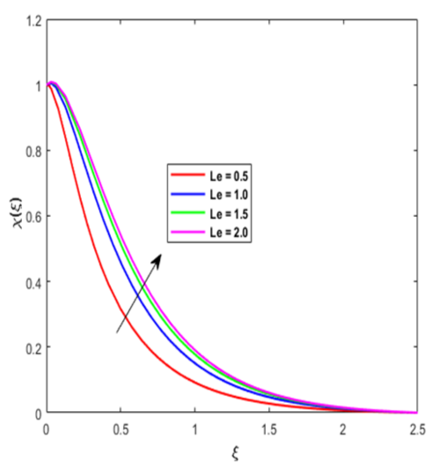

Fig 5. Stimulation of Lewis number $(Le = \mathbf{0.5}, \mathbf{1.0}, \mathbf{1.5}, \mathbf{2.0})$ on $\chi(\xi)$

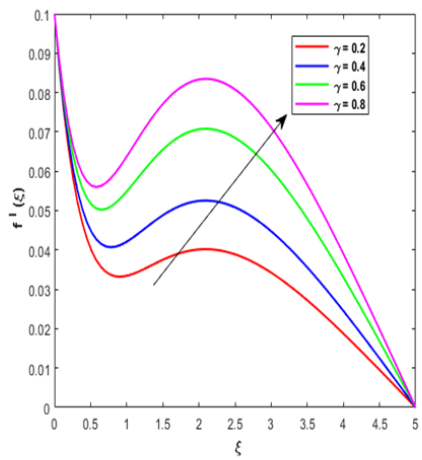

Fig 6. Stimulation of $(\gamma = \mathbf{0.2}, \mathbf{0.4}, \mathbf{0.6}, \mathbf{0.8})$ $on\ f^{'}(\xi)$

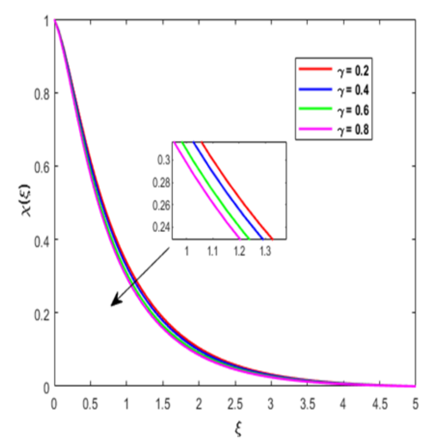

Fig 7. Influence of $(\gamma = \mathbf{0.2}, \mathbf{0.4}, \mathbf{0.6}, \mathbf{0.8})$ $on\ \chi(\xi)$

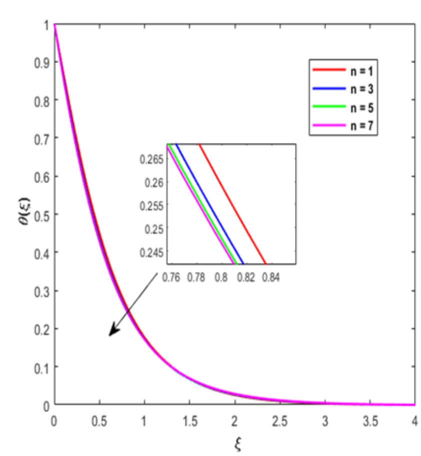

Fig 8. Stimulation of Chemical reaction parameter $(n = \mathbf{1}, \mathbf{3}, \mathbf{5}, \mathbf{7})$ $on\ \theta(\xi)$

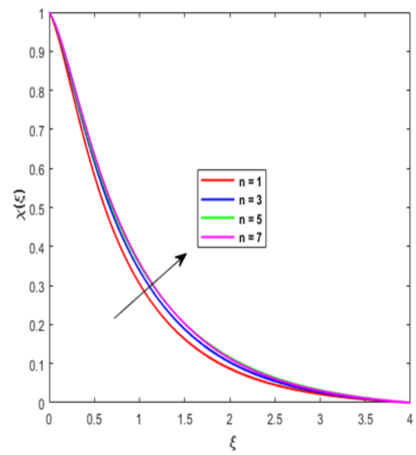

Fig 9. Stimulation of Chemical reaction parameter $(n = \mathbf{1},\mathbf{3},\mathbf{5},\mathbf{7})\ on\ \chi(\xi)$

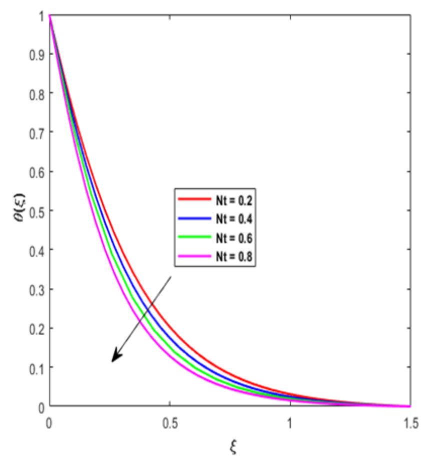

Fig 10. Stimulation of Thermoparasis parameter $(Nt = \mathbf{0.2},\mathbf{0.4},\mathbf{0.6},\mathbf{0.8})\ on\ \theta(\xi)$

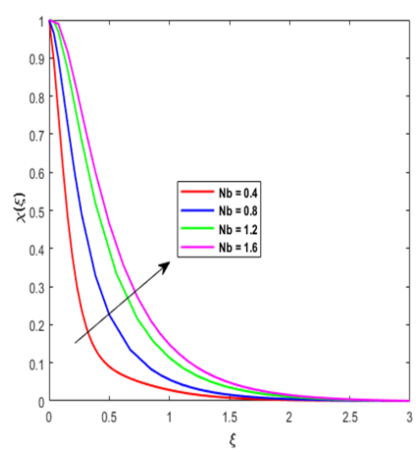

Fig 11. Stimulation of Brownian motion parameter $(Nb = \mathbf{0.4},\mathbf{0.8},\mathbf{1.2},\mathbf{1.6})\ on\ \chi(\xi)$

Higher values of radiation parameter (Nr) cause a descent in velocity (Figure 12) and concentration (Figure 13) fields with influence of parameter. Generally, more heat is released by thermal radiation to the flow near the surface. Concentration particles are drawn to cooler areas from the surface of the fluid, thereby elevating the temperature. The extended results are the advanced study of the impact of thermally radiation and buoyancy flow model with suspension of micro-organism strength and described on non-dimensional parameters.

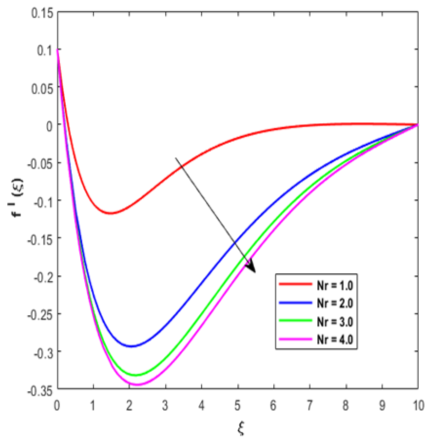

Fig 12. Stimulation of Thermal radiation $(Nr = \mathbf{1.0}, \mathbf{2.0}, \mathbf{3.0}, \mathbf{4.0})$ *on* $f^{'}(\xi)$

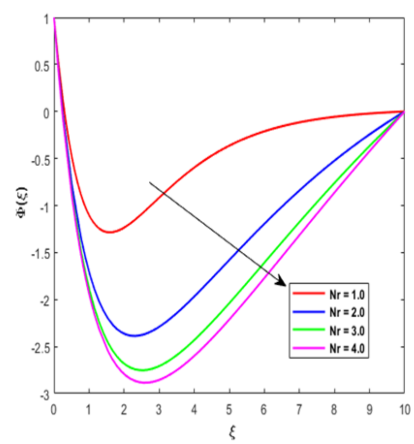

Fig 13. Stimulation of Thermal radiation $(Nr = \mathbf{1.0}, \mathbf{2.0}, \mathbf{3.0}, \mathbf{4.0})$ *on* $\phi(\xi)$

From Table 1 skin friction and Nusuult number results are discussed with the impact of enriching Hatman number $(Ha = 0.5, 1.0, 1.5, 2.0)$ on skin friction number $\left(Cf_x, Cf_y\right)$ has declined along the Nusellt number also declined. The influence of the Casson parameter on skin friction number $\left(Cf_x, Cf_y\right)$ has enhanced and in Nusellt number has declined. In chemical parameter has enhanced $(\delta = 0.3, 0.6, 0.9, 1.2)$ on skin friction number $\left(Cf_x, Cf_y\right)$ has enhanced and in Nusellt number has been declined. Impacts of Eckert number$(Ec = 0.1, 0.4, 0.8, 1.2)$ on skin friction number $\left(Cf_x, Cf_y\right)$ has declined and in Nusellt number has been enhanced.

Table 1. Assessment values of $(C_{\mathbf{fx}})$, $(C_{\mathbf{fy}})$ *and* $(Nu_{\mathbf{x}})$ **when** $Pr = \mathbf{3.5}$, $\delta = \mathbf{0.5}$, $K_{\mathbf{0}} = \mathbf{0.6}$, *and* $\phi_{\mathbf{1}} = \phi_{\mathbf{2}} = \phi_{\mathbf{3}} = \phi_{\mathbf{4}} = \mathbf{0.5}$

Ha	β	δ	*Ra*	*K*	*Ec*	*Da*	$C_{\mathbf{fx}}\,(Re_{\mathbf{x}})^{\mathbf{1/2}}$	$C_{\mathbf{fy}}\,(Re_{\mathbf{x}})^{\mathbf{1/2}}$	$Nu_{\mathbf{x}}(Re_{\mathbf{x}})^{-\mathbf{1/2}}$
0.5							-0.805351	0.035476	-0.007623
1.0							-0.822792	0.028740	-0.008147

Continued on next page

Table 1 continued

1.5							-0.843363	0.021878	-0.008555
2.0							-0.862619	0.016438	-0.008741
	0.1						-0.869142	0.027137	-0.007592
	0.3						-0.807109	0.025070	-0.008777
	0.5						-0.777182	0.024066	-0.009296
	0.7						-0.758562	0.023445	-0.009599
		0.3					-2.244415	0.120272	-0.011747
		0.6					-1.280824	0.052638	-0.009700
		0.9					-0.909852	0.030169	-0.008594
		1.2					-0.709021	0.019669	-0.007921
			1.1				-1.622021	0.073081	-0.008662
			2.2				-1.716039	0.077865	-0.007885
			3.3				-1.761513	0.080204	-0.007576
			4.4				-1.789869	0.081670	-0.007399
				0.2			-1.704111	0.012386	-0.007970
				0.4			-1.704210	0.049507	-0.007970
				0.6			-1.704636	0.111039	-0.007971
				0.8			-1.705758	0.195765	-0.007974
					0.1		-1.707110	1.210996	-0.008338
					0.4		-1.711646	1.170436	-0.008290
					0.8		-1.716069	1.131672	-0.008244
					1.2		-1.720377	1.094647	-0.008201
						1	-1.726831	1.040537	-0.008381
						3	-1.722482	1.076828	-0.008478
						6	-1.721374	1.086183	-0.008504
						9	-1.721004	1.089327	-0.008512

5 Conclusion

5.1 Novelty, Prospectus, and Recommendation

In this study, the consequence of bio-convection has been extensively considered due to its extensive collection of applications in transversely varied fields such as the manufacturing of aircraft, medicine, cosmetic production and modern defence systems. The impact of nonlinear partial derivative formulations is developed subjected to boundary layer theory. The foremost partial differential equations (PDE) are changed into an arrangement of ordinary differential equations by applying adequate corresponding transform. The outputs of these equations are performed numerically employing the RK method and computed well well-established BVP4C MATLAB software.

5.2 Importance of work

The present numerical study analyzes the buoyancy-driven flow of thermal and diffusive communication within the inundated Darcy medium. This study describes thermal radiation, thermophoresis, gyrotactic organisms and Brownian motion. This flow is analyzed in two circumstances, flow from place to place a cone and another one paraboloid.

The following concluding remarks can be drawn from the analysis.

1. Influence of Buoyancy parameter (Nc) and concentration (φ) the profile has opposite characteristics.
2. Lewis number gives rise to concentration (φ) and Micro-organism (χ).
3. Velocity and micro-organisms are higher via large values of γ.
4. Chemical reaction parameter declines the temperature and inclines micro-organisms.
5. Thermal radiation (Nr) consistently elevates on velocity and concentration profiles.

References

1) Reddy BN, Maddileti P. Casson nanofluid and Joule parameter effects on variable radiative MHD stretching sheet. *Partial Differential Equations in Applied Mathematics*. 2023;7:100487–100487. Available from: https://doi.org/10.1016/j.padiff.2022.100487.
2) Moatimid MG, Mohamed AM, Elagamy AK. Casson nanofluid flow within the conical gap between rotating surfaces of a cone and a horizontal disc. *Scientific Reports*. 2022;12:11275–11275. Available from: https://doi.org/10.1038/s41598-022-15094-w.

3) Hamid A. Terrific effects of Ohmic- viscous dissipation on Casson nanofluid flow over a vertical thin needle: buoyancy assisting and opposing flow. *Journal of Materials Research and Technology*. 2020;9(5):11220–11230. Available from: https://doi.org/10.1016/j.jmrt.2020.07.070.
4) Algahtani MA, Rafique K, Mahmood Z, Sinan RB, Hassan MUKA. MHD rotating flow over a stretching surface: The role of viscosity and aggregation of nanoparticles. *National Library of Medicine*. 2023;9(11). Available from: https//:doi.org/10.1016/j.heliyon.2023.e21107.
5) Reddy MV, Lakshminarayana P. Higher order chemical reaction and radiation effects on Magneto-hydrodynamic flow of a maxwell nanofluid with cattaneo-christov heat flux model over a stretching sheet in a porous medium. *Journal of fluids engineering*. 2022;144(4). Available from: https://doi.rg/10.1115/1.4053250.
6) Das UJ, Das M. Unsteady MHD rotating and chemically reacting fluid flow over an oscillating vertical surface in a darcian porous regime. *Frontiers in Heat and Mass Transfer*. 2021;17:1–8. Available from: https://doi.org/10.5098/hmt.17.18.
7) Gowda RJP, Al-Mubaddel, Fahad S, Kumar RN, Prasannakumara BC, Alibek I, et al. Computational modelling of nanofluid flow over a curved stretching sheet using Koo-Kleinstreuer and Li(KKL) correlation and modified Fourier heat flux model. *Chaos, Solitons and Fractals*. 2021;145:110774–110774. Available from: https://doi.org/10.1016/j.chaos.2021.110774.
8) Khan KA, Javed MF, M B Riaz. Heat and Mass transport analysis for Williamson MHD nanofluid flow over a stretched sheet. *Results in Physics*. 2023;53. Available from: https://doi.org/10.1016/j.rinp.2023.106873.
9) Adideen ZU, Saif RS. Impact of thermal radiation and internal heat generation on Casson nano-fluid flowing by a curved stretchable surface with suspension of carbon nanotubes (CNTS),. *Heliyon,* . 2023;9(8). Available from: https://doi.org/10.1016/j.heliyon.2023.e18941.
10) Sharma BK, Gandhi R, Mishra KN, Al-Mdallal MQ. Entropy generation minimization of higher order endothermic/exothermic chemical reaction with activation energy on MHD mixed convective flow over a stretching surface. *Scientific Reports*. 2022;12:17688. Available from: https://doi.org/10.1038/s41598-022-22521-5.
11) Gopal D, Jagadha S, Sreehari P, Kishan N, Mahendar D. A numerical study of viscous dissipation with first order chemical reaction and ohmic effects on MHD nanofluid flow through an exponential stretching sheet. *Materials Today: Proceedings*. 2022;59:1028–1033. Available from: https://doi.org/10.1016/j.matpr.2022.02.368.
12) Jagadha S, Gopal D, Kumar PV, Kishan N, Durgaprasad P. Three dimensional MHD nanofluid stagnation point flow with higher order chemical reaction. *Journal of Thermal Engineering*. 2022;8(2):286–298. Available from: https://doi.org/10.18186/thermal.1086264.
13) Rehman KU, Shatanawi W, Alharbi WAG, Shatnawi AMT. AI-Neural Networking Analysis (NNA) of thermally slip Magnetized Williamson (TSMW) fluid flow with heat wource, . *Case Studies in Thermal Engineering*. 2024;56. Available from: https://doi.org/10.1016/j.csite.2024.104248.
14) Ganesh GR, Sridhar W, Al-Farhany K, Ahmed ES. Electrically MHD Casson nanofluid flow and entropy exploration under the influence of the viscous dissipation, radiation and higher order chemical reaction. *Physica Scripta*. 2022. Available from: https://doi.org/10.1088/1402-4896/ac6e51.
15) Maas J, Mielke A. Modeling of chemical reaction systems with detailed balance using gradient structures. *Journal of statistical physics*. 2020;181:2257–2303. Available from: https://doi.org/10.1007/s10955-020-02663-4.
16) Basit MA, Tahir M, Shah NA, Tag SM, Imran M. An application to formable transform: Novel numerical approach to study the nonlinear oscillator. *Journal of Low Frequency Noise, Vibration and Active Control*. 2024;43. Available from: https://doi.org/10.1177/14613484231216198.
17) Basit MA, Imran M, Tahir M, Eladeb A, Kolsi L. Numerical analysis of mathematical model for heat and mass transfer through Bioconvective Maxwell nanofluid flow subject to Darcy-Forcheimer and Lorentz forces. *Int Journal of Heat and Fluid Flow*. 2024;106:109322–109322. Available from: https://doi.org/10.1016/j.ijheatfluidflow.2024.109322.
18) Farroq U, Basit MA, Fatima N, Albhushaybari A, din SME, Imran M, et al. Recent progress in Cattaneo-Christov heat and mass fluxes for bioconvectional Carreau nanofluid with motile microorganisms and activation energy passing through a nonlinear stretching cylinder. *Ain Shams Engineering Journal*. 2024;15(1):102316–102316. Available from: https://doi.org/10.1016/j.asej.2023.102316.
19) Basit MA, Imran M, Akgül A, Hassani MK, Alhushaybari A. Mathematical analysis of heat and mass transfer efficiency of bioconvective Casson nanofluid flow through conical gap among the rotating surfaces under the influences of thermal radiation and activation energy. *Results in Physics*. 2024;63:1–11. Available from: https://doi.org/10.1016/j.rinp.2024.107863.
20) Basit MA, Imran M, Safdar R, Tahir M, Ali MR, Hendy AS, et al. Thermally radiative bioconvective nanofluid flow on a wavy cylinder with buongiorno model: A sensitivity analysis using response surface methodology. *Case Studies in Thermal Engineering*. 2024;55:104178–104178. Available from: https://dx.doi.org/10.1016/j.csite.2024.104178.
21) Bhatti MM, Rashidi MM. Effects of thermo-diffusion and thermal radiation on Williamson nanofluid over a porous shrinking/stretching sheet. *Journal of Molecular Liquid*. 2020;16. Available from: https://doi.org/10.1016/j.molliq.2016.05.049.